SAND2014-19397R

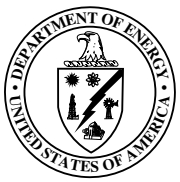

Sandia National Laboratories

Operated for the U.S. Department of Energy by

Sandia Corporation

Albuquerque, New Mexico 87185

date: November 3, 2014

to: Distribution

from: Edmundo Corona

subject: Numerical Simulations of Wave Propagation in Long Bars with Application to Kolsky Bar Testing.

1 Introduction

Material testing using the Kolsky bar, or split Hopkinson bar, technique has proven instrumental to conduct measurements of material behavior at strain rates in the order of 10^3 s^{-1}. Test design and data reduction, however, remain empirical endeavors based on the experimentalist's experience. Issues such as wave propagation across discontinuities, the effect of the deformation of the bar surfaces in contact with the specimen, the effect of geometric features in tensile specimens (dog-bone shape), wave dispersion in the bars and other particulars are generally treated using simplified models.

The work presented here was conducted in Q3 and Q4 of FY14. The objective was to demonstrate the feasibility of numerical simulations of Kolsky bar tests, which was done successfully. Prior to that kind of simulation, however, a series of exercises to demonstrate basic wave propagation phenomena in rods was carried out. The principal objective was to generate confidence in the numerical models. At the conclusion of Q4 simulations of wave shape modifications via pulse shapers were demonstrated. Further work has been funded for FY15 with the objectives of first comparing the results of simulations of compressive and tensile Kolsky tests against actual data and then to use numerical simulations to help with specimen design validation and data reduction.

2 Simulation of Basic Wave Propagation Phenomena in Rods

The first exercise to be discussed is shown schematically in Fig. 1(a). It consists of a steel striker bar of diameter $d_k = 0.25$ in. and length $l_k = 5$ in. at the left of the model traveling to the right with velocity $v_o = 133.5$ in/s. This bar impacts another steel bar of length $l = 144$ in. and diameter $d_1 = 0.25$ in. for the first 72 in. and $d_2 = 0.0938$ in. for the second 72 in. The axial stress history is monitored at points 1 and 2 in the bar as illustrated. Based on results of the wave equation[1], the impact should produce a rectangular pulse that propagates down the long bar with velocity

$$c = \sqrt{\frac{E}{\rho}},$$

where E and ρ are the Young's modulus and the density of the bar material, respectively. In the model, $E = 30 \times 10^6$ psi and $\rho = 7.48 \times 10^{-4}$ slug-ft/in^4, giving $c = 200,267$ in/s. According to the wave equation, the pulse velocity is independent of pulse shape and amplitude. The signed amplitude of the stress pulse is given by

$$\sigma = -E\frac{v_o}{2c}.$$

The length of the pulse is $2l_k$, which gives it a time duration of

$$T = \frac{2l_k}{c}.$$

In the case being considered here, $\sigma = 10$ ksi and $T = 0.05$ ms.

Because of the mismatch in impedance at the diameter step, part of the pulse is transmitted, and part of the it is reflected at the discontinuity. The amplitudes of the transmitted and reflected stress pulses are given by

$$\sigma_t = \frac{2d_1^2}{d_1^2 + d_2^2}\sigma_i$$

and

$$\sigma_r = \frac{d_2^2 - d_1^2}{d_1^2 + d_2^2}\sigma_i.$$

Here, σ_i is the signed amplitude of the stress pulse incident onto the diameter step. The transmitted pulse has the same sign as the incident pulse while the sign of the reflected pulse will have sign opposite to the incident one if the diameter drops, as in Fig. 1(a). Substituting the values $d_1 = 0.125$ in., $d_2 = 0.09375$ in. and $\sigma_i = -10$ ksi gives $\sigma_t = -12.8$ ksi and $\sigma_r = 2.8$ ksi

[1]See Graff, K.F., Wave Motion in Elastic Solids, Oxford University Press, 1975. Chapter 2. Reprinted by Dover Publications, New York, 1991.

The finite element model of the problem assumed axisymmetry and was constructed within the framework of the commercial finite element code Abaqus/Explicit. CAX4R elements, which are four-node, axisymmetric continuum elements with reduced integration and hourglass control were used throughout the model. It was found that relatively coarse meshes gave reasonable results. The discretization of the case being considered included elements of size 1/32 in. on the side. To complete the description of the isotropic elastic model, the Poisson ratio was set to $\nu = 0.3$.

Figure 1(b) shows the stress traces with respect to time at points 1 and 2 in the model. The wave speed can be obtained given the distance between these points and the time interval between the arrival of the pulses. Based on the data the value is $c = 200 \times 10^3$ in/s, which agrees with the value calculated from the material properties. Note that the stress pulse has an initial mean amplitude of 10 ksi and duration of 0.05 ms, as expected. The shape of the pulse is nearly rectangular, but exhibits high frequency oscillations. This is a well-known effect caused by dispersion, which in a rod causes signals of higher frequency to propagate at a slower speed. Clearly, some of the high frequency content of the main pulse fell behind and arrived at point 1 after the main pulse. This loss of high frequency content gives the "ringing" behavior in the pulse. Dispersion in rods is the result of the lateral inertia that is excited by Poisson's ratio. Indeed, setting $\nu = 0$ in the simulation eliminated this ringing.

The pulse transmitted to the smaller diameter bar is shown in red in the figure as detected at point 2. The predicted pulse signed amplitude calculated above is 12.8 ksi and this is reflected in the simulation. Similarly the predicted amplitude of the reflected pulse is -2.8 ksi, and that corresponds to the mean amplitude shown in Fig. 1(b).

Figures 2 (a) and (b) show a similar case, but now the part of the bar to the right of the step has larger diameter. The results are in general similar as discussed above, with the difference that now the stress amplitude of the transmitted pulse is smaller than that of the incident pulse and the reflected pulse as calculated at point 1 has the same sign as the initial pulse. The predicted mean signed amplitudes of the transmitted and reflected pulses were $\sigma_t = -7.8$ ksi and $\sigma_r = -2.2$ ksi respectively, and these are reflected well in the numerical predictions.

3 Effect of Sharp Mesh Refinements on Wave Propagation

The next exercise concentrated on investigating the effect of a relatively sharp mesh refinement in a finite element model of a rod. This type of mesh transition may be necessary in cases where a Kolsky bar test is being simulated in order to make computations more efficient. Changing the element size, however, may affect the local stiffness of the model with the possibility of causing reflections and amplitude changes of the transmitted pulses. Figure 3(a) shows the model used to study this. It is similar to the previously considered models, but the diameter of all rods is a constant 0.75 in. This diameter is more typical of Kolsky bar set-ups than the 0.25 in. used above. Note that the striker bar has the same length as before. The initial velocity in this case was $v_o = 267$ in/s, thus giving rise to a stress pulse with amplitude of 20 ksi in the longer bar. The longer bar contains a region

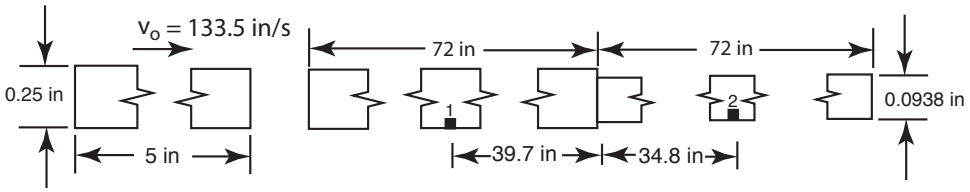

(a)

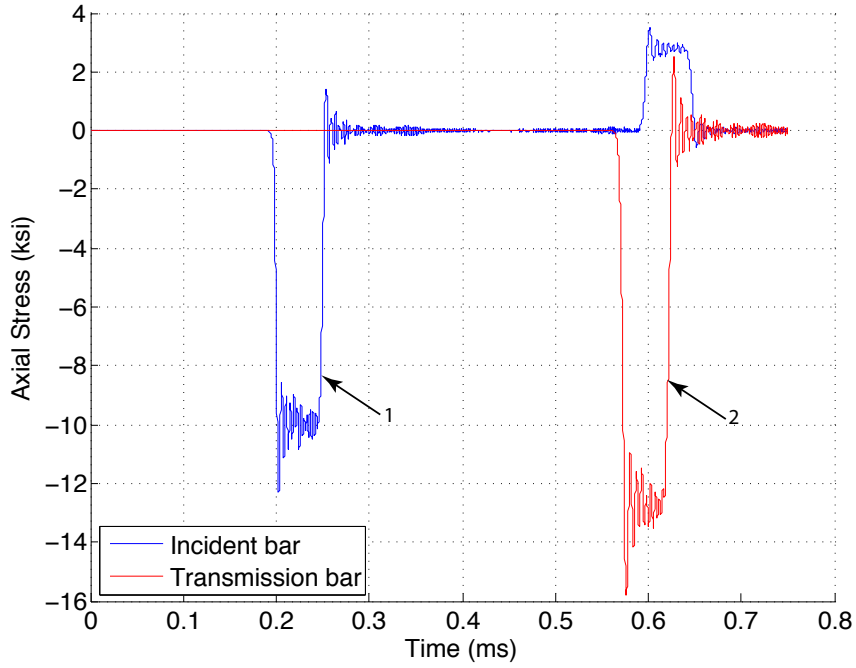

(b)

Figure 1. (a) Geometry of a bar of circular section that steps down in area used in the numerical calculations and (b) calculated incident and transmitted stress histories measured at locations 1 and 2 in (a).

A and a region B of equal lengths. Figure 3(b) shows the results of three simulations: one with a uniformly coarse mesh in both A and B with four elements through the radius, one with a uniformly fine mesh with 24 elements through the radius and the last where the rod model transitions from 4 elements through the radius in A to 24 elements in B as shown in Fig. 4. Overall, the three responses are virtually indistinguishable as seen in Fig. 3(b). Note how dispersion reduced the number of ripples in the stress signals between points 1 and 2. Figures 5 (a) and (b) show the details of the peaks of the stress calculations at points 1 and 2 respectively. Note that some small differences between the three cases can be seen at this level of magnification. These should not be consequential in the simulation of Kolsky bar tests. One interesting issue is that if one examines the stress calculated at point 1, it is easy to see that the coarse and the stepped mesh cases give slightly different results. This indicates that the presence of the fine mesh ahead of the stress pulse influences the calculations in the coarse region, a fact that was surprising.

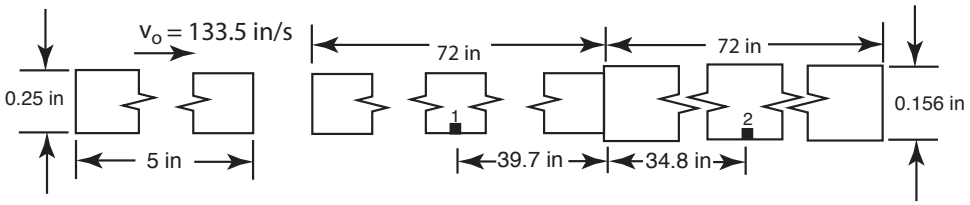

(a)

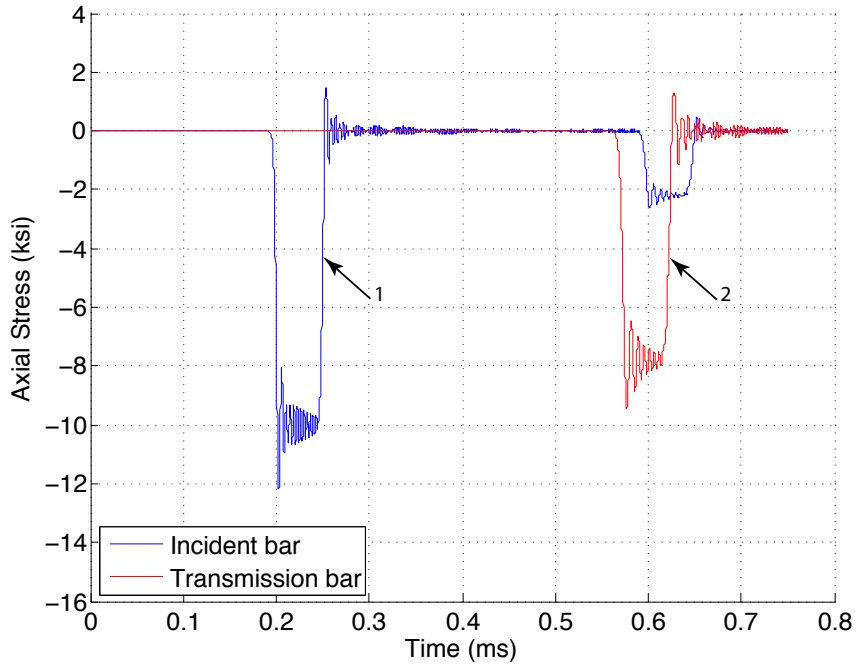

(b)

Figure 2. (a) Geometry of a bar of circular cross-section that steps up in area used in the numerical calculations and (b) calculated incident and transmitted stress histories measured at locations 1 and 2.

4 Simulation of a Compressive Kolsky Bar Test

The next exercise consisted of the simulation of a compressive Kolsky bar test. The dimensions of the bars and the specimen are shown in Fig. 6(a). The striker bar initial velocity was 267 ft/s. The amplitude of the strain pulse is therefore 6.67×10^{-4}. The specimen is taken to have a uniaxial true stress-strain that is elastic-perfectly plastic with a yield stress of 40 ksi, which translates into the engineering stress-strain curve shown in red in Fig. 6 (c). The coefficient of friction between all contact surfaces was $\mu = 0$. The strain calculated at point 1 in the incident bar A is ε_i. It is later followed by the reflected pulse ε_r at the same location. The strain calculated at point 2 in the transmission bar is ε_t. The strain traces at both points are shown in Fig. 6(b). The engineering stress and strain in the specimen (σ_s

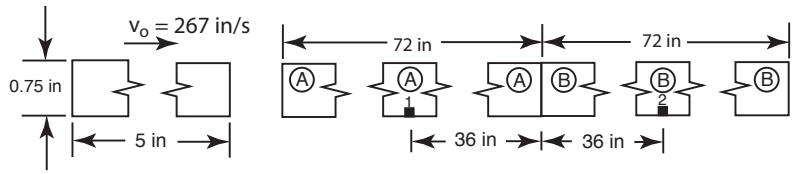

(a)

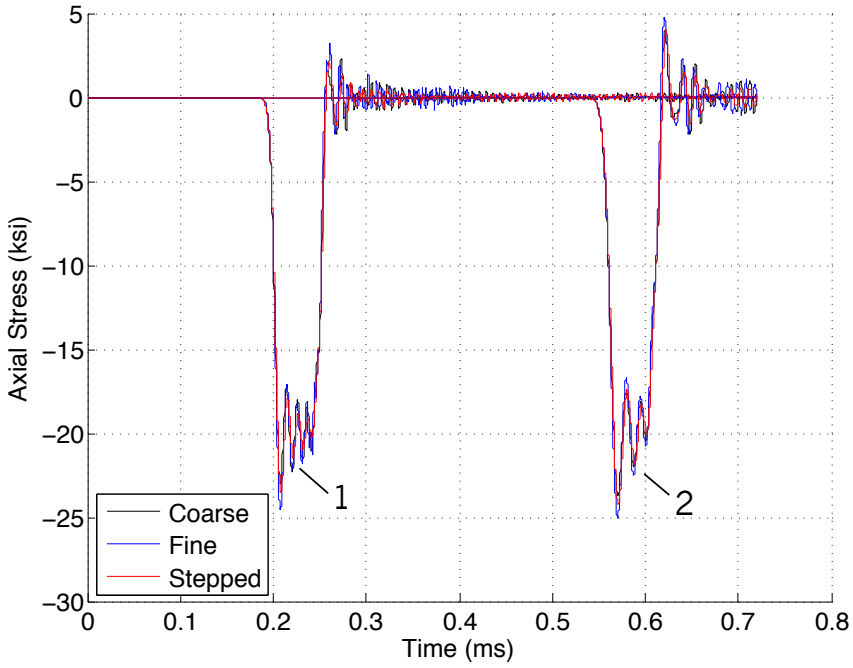

(b)

Figure 3. (a) Geometry of a bar model with circular cross-section with a mesh transition from coarse in A to fine in B in the "stepped" case and (b) calculated stress histories at points 1 and 2.

and ϵ_s can be calculated from the expressions given by Graff,

$$\sigma_s = \frac{EA\varepsilon_t}{A_s}$$

and

$$\varepsilon_s = -\frac{2c}{l_s}\int_0^t \varepsilon_r \, d\tau,$$

where A is the cross-sectional area of the incident and transmitted bars. A_s and l_s are the cross-sectional area and length of the specimen. The predicted engineering stress-strain curve for the specimen material is shown in blue line in Fig. 6(c). The wavy character of the stress response is attributed to the characteristics of the incident wave, which had been influenced by the effects of dispersion. Note that while the engineering stress-strain curve

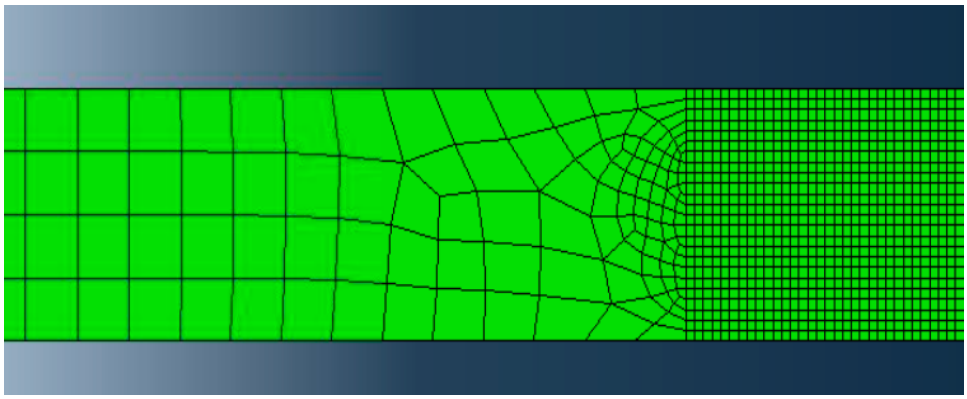

Figure 4. Detail of the transition between coarse mesh in A to a fine mesh in B.

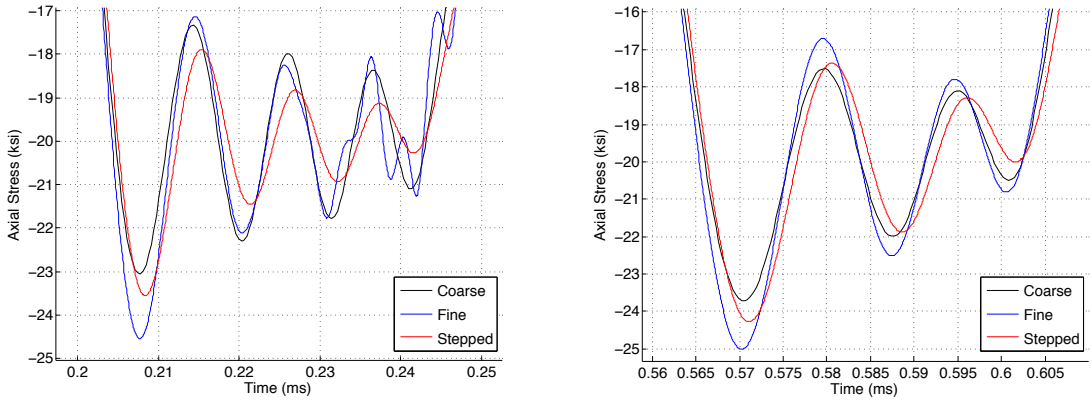

Figure 5. Detail of the stress oscillations for the three cases considered in Fig. 3. (a) At location 1 and (b) at location 2.

of the material is not predicted well prior to yielding (this is common in actual Hopkinson bar testing and needs to be investigated), the plastic response is predicted rather well by the average of the calculated curve. A strain of only 8% was achieved in the specimen because the striker bar had a short length. In actual Kolsky tests, striker bars usually have lengths between 12 and 24 in. Figure 7 shows the final distribution of equivalent plastic strain (PEEQ) in the specimen. It shows a variation between 7.9 and 8.2%.

5 Pulse Shapers

The last exercise conducted in FY14 simulated the effect of including a pulse shaper on the characteristics of the pulse propagated in a rod. A pulse shaper consists of a small material disk located at the impact site between the striker bar and the incident bar in a Kolsky test. Its purpose is to modify the shape of the wave produced by the impact and optimize it for the purposes of a particular test. In the case considered here, the model included an

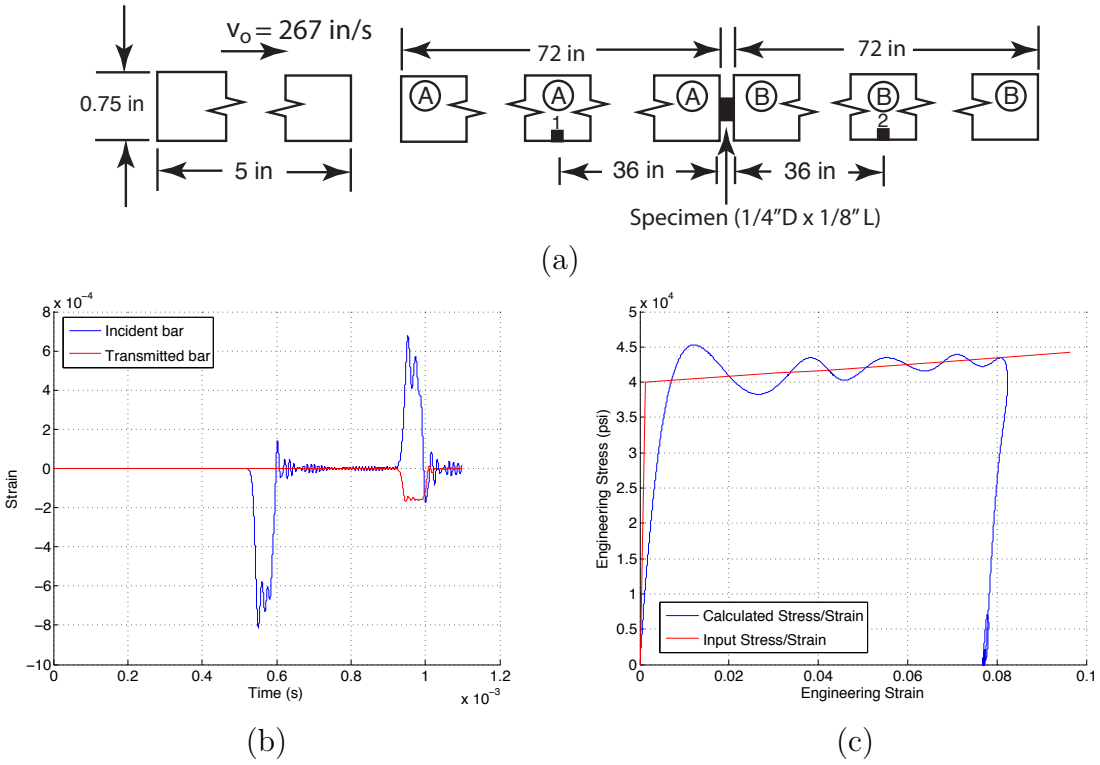

Figure 6. Computational results for simulation of Kolsky bar compression specimen. (a) Model schematic, (b) strain vs. time histories at point 1 in the incident pulse bar and a point2 in the transmitted pulse bar and (c) comparison between the engineering stress-strain curve inputted to the model and the calculated stress-strain curve from the bar strain data.

elastic-plastic disk with the dimensions shown in Fig. 8(a) and properties of annealed copper. The initial velocity of the striker bar was 133.5 ft/s, nominally giving a 10 ksi stress pulse in the absence of the pulse shaper. Figure 8(b) shows the results of the exercise and includes predictions of the stress pulse by the three models at the locations 1 and 2 indicated in Fig. 8(a). The labels "Coarse" and "Fine" refer to the size of the finite element mesh. The coarse mesh had four elements through the radius of the bars and 8×3 elements along the radius and length of the pulse shaper, while the fine mesh had eight elements through the radius of the bars and 16×5 elements in the pulse shaper. All elements had aspects ratios near one. While the mesh size has some effects on the results, it did not seem to significantly affect the stress histories as shown in Fig. 8(b).

The third prediction is for impact without the pulse shaper. As before, the results show a square pulse displaying the effects of dispersion. The effects of including the pulse shaper are clearly seen. The rise and decay times of the stress wave are increased quite a bit and the shapes are similar to that of the response of a first-order system. Note that the duration of the stress pulse is also increased significantly, and that the stress oscillations due to dispersion are significantly suppressed. The predicted effect of the pulse shaper on the response of specimens in Kolsky bar tests will be investigated in FY15.

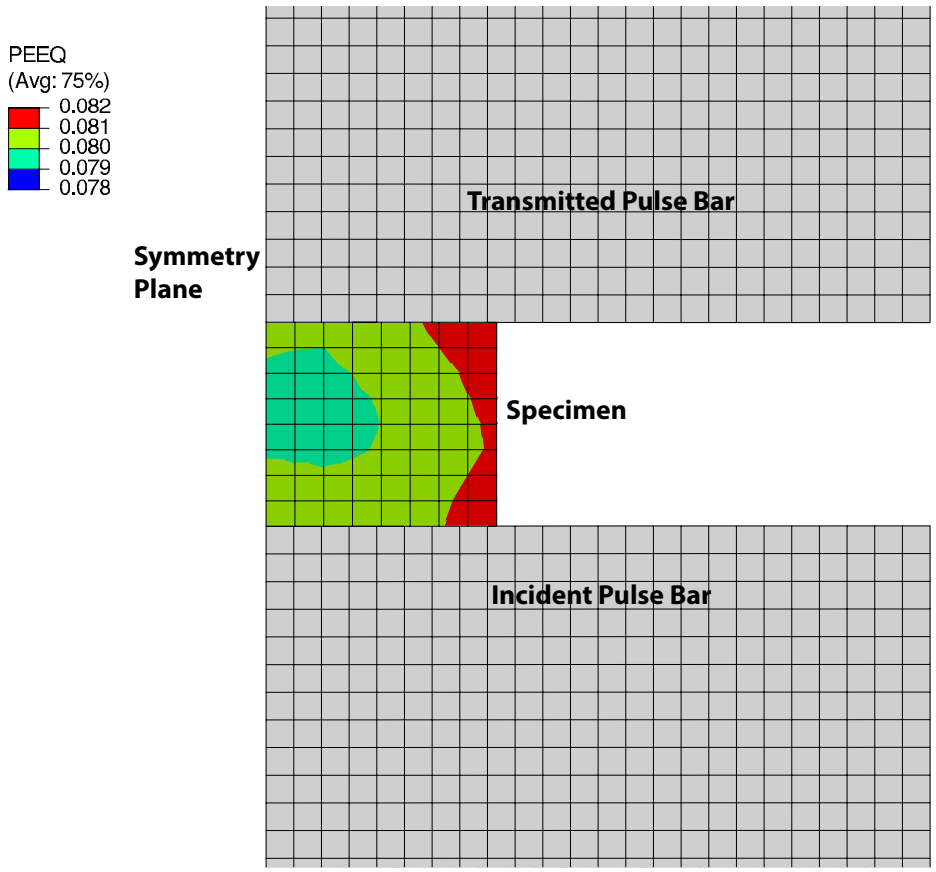

Figure 7. Equivalent plastic strain distribution in specimen after the stress wave passed.

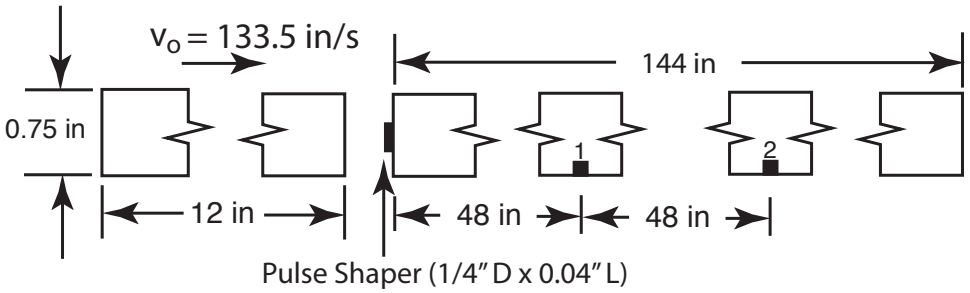

(a)

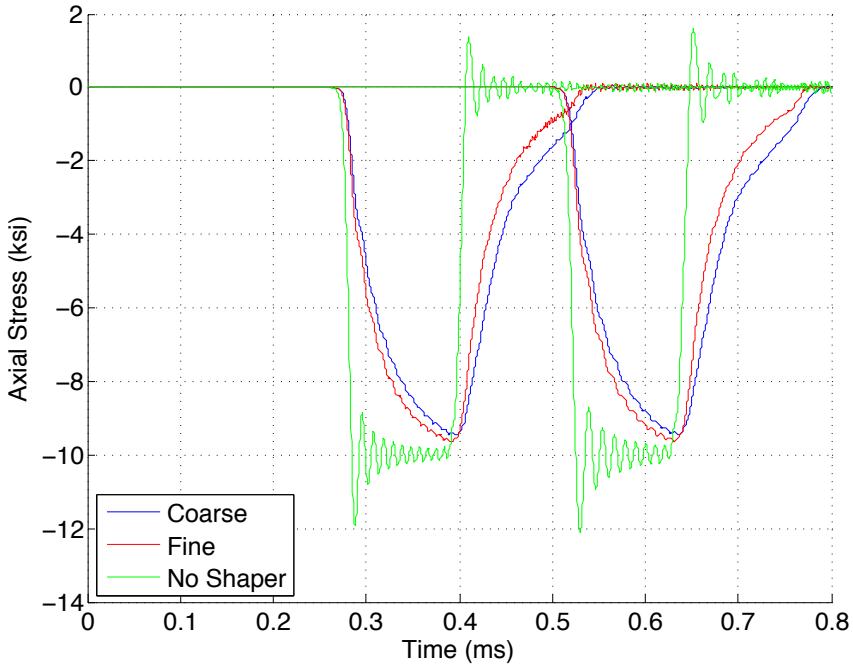

(b)

Figure 8. (a) Geometry of the model used to study the effect of pulse shapers and (b) stress histories at two points on a bar with a pulse shaper between the striking bar and the transmission bar. Results are shown for two mesh densities and they are compared against the wave profile produced without a pulse shaper.

6 Conclusions

The exercises conducted during Q3 and Q4 of FY14 demonstrated that axisymmetric finite element models of wave propagation in bars provide an excellent place to start more serious investigations into the design and data reduction of Kolsky bar material tests. Clearly, one can think of situations where axisymmetry may not be appropriate, such as apparatus misalignment, specimens that are not axisymmetric, etc. These are situations that can also be addressed by more sophisticated (and expensive) finite element modeling. For the immediate future, much can be learned and applied to design from the consideration of nominally perfect tests that can be studied with axisymmetric models.

The next steps of the project include:

- Simulation of actual Kolsky bar compression tests and comparison with experimentally acquired data in order to validate the finite element model.
- Study of the effect of specimen geometry, friction and pulse shapers on the test results and, in conjunction with experimental results, establish test design guidelines.
- Simulation of Kolsky bar tensile tests and study of the effect of various factors on the test results. Similar to the above, the objective will be to establish design guidelines for tensile testing.
- Design optimization of the long pulse "dropkinson bar" that is currently being constructed.

Sandia National Laboratories is a multi-program laboratory managed and operated by Sandia Corporation, a wholly owned subsidiary of Lockheed Martin Corporation, for the U.S. Department of Energy's National Nuclear Security Administration under contract DE-AC04-94AL85000.

Internal Distribution:

1	0557	D. Croessmann	1520
1	0557	D. Epp	1522
1	0557	B. Song	1558
1	0557	D. Jones	1558
1	0815	J. Johannes	1500
1	0840	J. Redmond	1550
1	0840	E. Corona	1554
1	0840	H. Fang	1554